Journal of Power Sources 242 (2013) 865–871

Contents lists available at SciVerse ScienceDirect

Journal of Power Sources

journal homepage: www.elsevier.com/locate/jpowsour

In-situ synthesis of carbon coated Li_2MnSiO_4 nanoparticles with high rate performance

Dan Sun [a], Haiyan Wang [a,*], Ping Ding [a], Nan Zhou [a], Xiaobing Huang [b], Shuai Tan [a], Yougen Tang [a]

[a] Key Laboratory of Resources Chemistry of Nonferrous Metals, Ministry of Education, School of Chemistry and Chemical Engineering, Central South University, Changsha 410083, PR China
[b] College of Chemistry and Chemical Engineering, Hunan University of Arts and Science, ChangDe 415000, PR China

HIGHLIGHTS

- *In-situ* coating approach using phenolic resin as carbon source is introduced for Li_2MnSiO_4/C composite.
- A thin and homogeneous carbon layer with high sp^2/sp^3 ratio, as well as the limited particle size is achieved.
- The carbon-coated Li_2MnSiO_4 using phenolic resin as carbon source exhibits high rate performance.

ARTICLE INFO

Article history:
Received 18 February 2013
Received in revised form
24 May 2013
Accepted 26 May 2013
Available online 5 June 2013

Keywords:
Li-ion battery
Lithium manganese silicate
In-situ carbon coating
Phenolic resin
Nanoparticles
Rate performance

ABSTRACT

In-situ coating approach using phenolic resin as carbon source is introduced in this work with the aim of getting high rate Li_2MnSiO_4/C composite. Li_2MnSiO_4/C nanoparticles, average diameter of *ca.* 25 nm, are well dispersed and the carbon layers are 3–8 nm in thickness. The composites deliver much higher electrochemical performance than those using sucrose as carbon source, in terms of reversible discharge capacity and cycling performance. High rate performance is also observed. It exhibits high reversible capacities of 181.6, 149.1, 133.5 mAh g^{-1} at 0.4, 1.2 and 2 C, respectively. At 4 C-rate, the electrode still maintains a discharge capacity of 108.7 mAh g^{-1}, around 52.5% of its capacity at 0.1 C. Apparently, *in-situ* synthesis of carbon coated Li_2MnSiO_4 using phenolic resin as carbon source results in thin and homogeneous carbon layer with relatively high sp^2/sp^3 ratio, as well as the limited particle size, which are the main reasons for the superior rate capability.

1. Introduction

Over the past two decades, there has been great interest in development of new high-capacity cathode materials for Li-ion battery as part of the ongoing efforts to meet the requirement of next generation rechargeable batteries for electrical vehicle [1–5]. The commercial Li-ion battery mainly involves the use of a layered structure transitional metal oxide, e.g. $LiCoO_2$ as positive electrode material. However, $LiCoO_2$ shows severe limitations in terms of low available capacity (only 140 mAh g^{-1}), high cost, toxicity and safety [1,6].

$(XO_4)_n^-$ polyanion compounds have attracted lots of attention for its unique properties as Li-ion battery cathode [3,7–9]. Of these materials, the olivine lithium iron phosphate ($LiFePO_4$) has been widely studied from both scientific and technical points of view, due to its excellent structure and thermal stability, as well as inexpensive and environmental benign characteristics [7,10]. Despite these advantages, it suffers from the low electronic conductivity. To address such problem, numerous strategies including cationic doping [11,12], carbon coating [7] and synthesizing nanostructural particles [13] have been utilized. Nevertheless, energy density of $LiFePO_4$ is relatively limited partially due to only one lithium ion extraction from the host theoretically. With this regard, the orthosilicate family of Li_2MSiO_4 [3,14–17], where M is some transition-metals Fe, Mn or Co, are becoming interesting candidate for Li-ion battery by virtue of their potential ability to facilitate the extraction of more than one lithium ion per transition metal.

* Corresponding author. Tel.: +86 731 88830886; fax: +86 731 88879616.
E-mail address: wanghy419@csu.edu.cn (H. Wang).

0378-7753/$ – see front matter © 2013 Elsevier B.V. All rights reserved.
http://dx.doi.org/10.1016/j.jpowsour.2013.05.143

Among them, a reversible capacity of ~150 mAh g^{-1} with stable cycling life could be demonstrated for Li_2FeSiO_4 [3,18]. However, like the $LiFePO_4$, Li_2FeSiO_4 also shows the limited energy density owing to the Fe^{2+}/Fe^{3+} redox couple. In theory, two lithium ions could be extracted from Li_2MnSiO_4, corresponding to Mn^{2+}/Mn^{3+} and Mn^{3+}/Mn^{4+}, which results in the theoretical capacity of 333 mAh g^{-1} [19–24]. Besides, operating voltage (>4.2 V) for Li_2MnSiO_4 is relatively higher than that of Li_2FeSiO_4.

Till now, only a few reports have mentioned the electrochemical characterization of Li_2MnSiO_4 because of their tendency to become the amorphous after the extraction of Li ions [14,19,22–24]. The structural instability results in very poor cycling performance. Meantime, the electronic conductivity of pure Li_2MnSiO_4 is around 10^{-14} S cm^{-1} at room temperature, which makes it almost electrochemical inactive [15]. Li et al. prepared the carbon coated Li_2MnSiO_4 by a solution method followed a solid state process, which showed a high initial discharge capacity of 209 mAh g^{-1} [22]. However, the as-prepared material without carbon only delivered a very low discharge capacity of 10 mAh g^{-1}. Dominko et al. [25] found that only 0.6 Li could be extracted in the initial charge process. At the 5th cycle, only 0.3 Li could be reversible deintercalated. Carbon coating is considered as a very potential strategy to improve the electrochemical performance of Li_2MnSiO_4. Note that the carbon sources and coating methods greatly affect the electrochemical performance. Two-step processes were often used for carbon coating, in which carbon source was mixed with the precursor solid by ball milling, leading to heterogeneous coating [22,26]. Additionally, severe aggregation of the particles appeared during the milling. There is no doubt that *in-situ* carbon coating would form a thin and homogeneous carbon layer on the surface of particles and thus contribute to good electrochemical properties. Aravindan et al. [19] employed an adipic acid assisted sol–gel route to synthesize Li_2MnSiO_4/C composite, which delivered relatively good cycling stability.

Much work has suggested that the selected carbon precursors directly affect the characteristics of the carbon additive, in terms of its structure, distribution and thickness of carbon coating layer, which are proportional to the performance of C-coated composite electrode [27–30]. Doeff et al. found that the increased sp^2-coordinated carbon promised better electrochemical performance for $LiFePO_4$ [31,32]. Functionalized aromatic or ring-forming organic precursor has received considerable attention as carbon source for electrode materials [27,31,33]. Accordingly, well carbon-coated Li_2MnSiO_4 composite with the average diameter of *ca.* 25 nm was synthesized in this work by *in-situ* coating approach using phenolic resin as carbon source. Nanoscaled electrode material with the high surface area is favorable for the high-rating and maximizing the interfacial contact between the active particles and the surrounding electrolyte [34]. To the best of our knowledge, the as-prepared Li_2MnSiO_4/C composite exhibited the highest rate performance to date.

2. Experimental

A stoichiometric amount of lithium acetate dehydrate (Sigma–Aldrich, reagent grade, 98%), manganese acetate tetrahydrate (Sigma–Aldrich, reagent grade, 99%) and $Si(OC_2H_5)_4$ (TEOS, Sigma–Aldrich, reagent grade, 98%) were dissolved in ethanol and the mixed solution was stirred at 80 °C using a reflux cooling system. One hour later, a certain amount of phenolic resin powder (provided by BTR Battery Materials Co., Ltd), which could be dissolved in ethanol was added as carbon source. After refluxing at 80 °C for 24 h, the solvent was evaporated at 100 °C to form the xerogel. The resulting precursor was finely ground by agate mortar and then pressed into pellets and calcined at 600 °C for 10 h under a mixed flowing H_2/Ar (5:95 by volume). The as-prepared product was denoted as Li_2MnSiO_4/C (RF)-600. The samples calcined at 650 and 700 °C were also obtained by the similar preparation method, denoted as Li_2MnSiO_4/C (RF)-650 and Li_2MnSiO_4/C (RF)-700, respectively.

For comparison, Li_2MnSiO_4/C using sucrose as carbon source was also prepared as following procedures: a stoichiometric amount of lithium acetate dehydrate (Sigma–Aldrich, reagent grade, 98%), manganese acetate tetrahydrate (Sigma–Aldrich, reagent grade, 99%) and $Si(OC_2H_5)_4$ (TEOS, Sigma–Aldrich, reagent grade, 98%) were dissolved in ethanol and the mixed solution was stirred at 80 °C using a reflux cooling system. Twenty four hours later, the ethanol was evaporated at 100 °C to form the dried gel. Then it was ground by agate mortar. As follows, a certain amount of the precursor was milled with sucrose in acetone. After evaporating of acetone, the mixture was pressed into pellets and heated to 600 °C for 10 h under a mixed flowing H_2/Ar (5:95). The as-prepared material was denoted as Li_2MnSiO_4/C (SR).

By Vario EL III instrument (ELEMENTAR), the carbon contents of the as-prepared Li_2MnSiO_4/C using phenolic resin and sucrose as carbon sources were determined to be 8.89% and 8.11%, respectively. The specific capacities of the as-prepared materials in this work were calculated with the mass of Li_2MnSiO_4. Powder X-ray diffraction (XRD) data were collected by a Stoe STADI/P diffractometer operating in the transmission mode and utilizing a Fe-Kα1 source (λ = 1.936 Å). X-ray diffraction data of electrode powder after different cycles were examined on a Stoe STADI/P diffractometer. The electrode powder consisting of active material, super S carbon and binder was assembled into a capillary with the diameter of 7 mm and then sealed to protect the charged active material. The related operations were carried out in an Ar-filled MBraun glove box. Morphological studies were conducted using a JEOL JEM-2100F transmission electron microscopy (TEM) with an accelerating voltage of 200 keV. N_2 adsorption–desorption analysis was carried out using a Micromeritics Tristar 3020. The typical sample weight used was about 100 mg. The outgas condition was set to 180 min at 120 °C under vacuum, and all adsorption–desorption measurements were carried out at liquid nitrogen temperature. Raman spectrum was tested with LabRAM Aramis (HORIBA Jobin Yvon) spectrometer. Four-point probe method (Suzhou Tongchuang, SZT-2B) was employed to measure the electronic conductivity for samples using phenolic resin or sucrose as carbon sources.

Cathodes were constructed by mixing the active material, polyvinylidene fluoride (PVDF), and super S carbon in the weight ratio of 80:10:10. Tetrahydrofuran was used as solvent. The slurry was cast onto Al foil using the Doctor-Blade technique. After solvent evaporation at room temperature and heating at 80 °C under

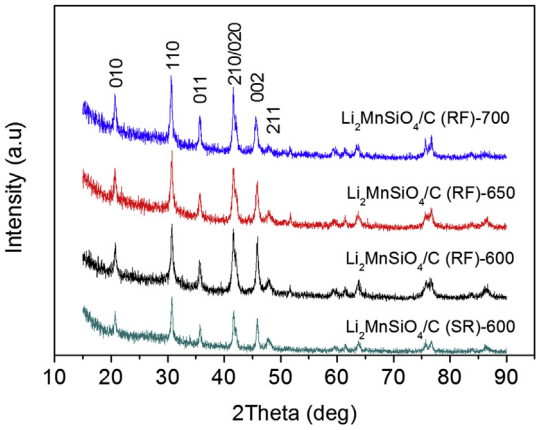

Fig. 1. XRD patterns of as-prepared Li_2MnSiO_4/C (RF) composites at various temperatures: 600 °C; 650 °C; 700 °C, associated with Li_2MnSiO_4/C (SR)-600.

Table 1
Lattice parameters of as-prepared Li_2MnSiO_4/C under different conditions.

Samples	*a* (nm)	*b* (nm)	*c* (nm)	*V* (nm^3)
Li_2MnSiO_4/C (RF)-600	0.6321	0.5367	0.4963	168.39
Li_2MnSiO_4/C (RF)-650	0.6304	0.5375	0.4965	168.23
Li_2MnSiO_4/C (RF)-700	0.6296	0.5373	0.4971	168.16
Li_2MnSiO_4/C (SR)-600	0.6303	0.5373	0.4969	168.29

vacuum for 8 h, the electrodes were assembled into coin-type cells with a lithium electrode (99.9%, Aldrich) and LP-30 electrolyte (Merck; 1 M $LiPF_6$ in 1:1 v/v ethylene carbonate/dimethyl carbonate). The loading mass of each electrode ranges from 2 to 3 mg cm^{-2}. The cells were constructed in an Ar-filled MBraun glove box and cycled galvanostatically between 1.5 and 4.8 V or 4.5 V (voltage unit in this paper is versus Li/Li^+) at a desired current density using a MACCOR Series 4200 cycler at 30 °C. Cyclic voltammetry (CV) measurement was operated using a Biologic VMP3 Multichannel Workstation (Bio-Logic SAS) with a scan rate of 0.1 mV s^{-1} between 1.5 and 4.8 V at room temperature.

3. Results and discussion

Fig. 1 presents the XRD patterns of the Li_2MnSiO_4/C (RF) composites prepared at various temperatures. As can be seen, all three samples demonstrate the similar XRD patterns, which are well indexed to Li_2MnSiO_4 phase with orthorhombic structure ($Pmn2_1$ space group) [22]. It is well known that Li_2MnSO_4 exhibits rich crystal chemistry owing to its complex polymorphisms. At least three kinds of polymorphs ($Pmn2_1$, *Pmnb* and $P2_1/n$ space groups) were often involved for Li_2MnSiO_4 depending on the annealed temperatures [35–38]. From the XRD pattern results, in this work, only the $Pmn2_1$ phase could be easily found, indicating the high purity of as-prepared material after sintering during 600–700 °C. The lattice parameters of $a = 0.6321(3)$ nm, $b = 0.5367(2)$ nm, $c = 0.4963(1)$ nm are calculated for the sample prepared at 600 °C, which are in close agreement with those reported values [22]. Table 1 gives the lattice parameters of Li_2MnSiO_4/C under different conditions. As observed, increasing the sintering temperature would slightly compress the crystal volume. And the XRD pattern of Li_2MnSiO_4/C (SR) prepared at 600 °C is also presented in Fig. 1, indicating the relatively pure phase of Li_2MnSiO_4 with the space group of $Pmn2_1$.

Electrochemical performance of Li_2MnSiO_4/C (RF) composites sintered at various temperatures was compared in Fig. 2. All three samples show the similar cycling instability, with large capacity loss in the first 20 cycles. Such phenomenon agrees well with the reported results, which should be mainly originated from the structural transformation from crystalline into amorphous phase [22,26,39]. Note that the capacity fading then becomes slow, especially for that prepared at 600 °C. An initial discharge capacity of 204.6 mAh g^{-1} is observed for the sample prepared at 600 °C. The stated specific discharge capacity represents the extraction of 1.23 lithium ions per formula unit, which is a considerable value at 30 mA g^{-1}. However, after 40 cycles, the discharge capacity decreases to 70.7 mAh g^{-1}, corresponding to only 0.43 reversible lithium ions. It is apparent that increasing the sintering temperature did not improve the cycling stability, but gave the slight lower capacity, which might be resulted from the tiny crystal volume contraction. The first load curves of the three samples, Fig. 2(b), display the similar charge capacity, but the Coulombic efficiency is reduced with the increasing of the sintering temperature. Therefore, the following Li_2MnSiO_4/C (RF) is the one calcined at 600 °C unless otherwise specified.

Morphological features of as-prepared Li_2MnSiO_4/C (SR) and Li_2MnSiO_4/C (RF) are shown in Fig. 3. It can be seen that Li_2MnSiO_4/C (SR) exhibits much larger particle size (30–50 nm) and severe particle aggregation. Large bulk carbon could be easily observed in Fig. 3(a, b), indicating the poor coating for the two-step method. On the contrary, Li_2MnSiO_4/C (RF) is well distributed. Apparently, *in-situ* carbon coating using phenolic resin gives much better carbon coated Li_2MnSiO_4 with smaller primary particle diameter of *ca.* 25 nm. According to the Scherrer's equation, the average crystalline size of Li_2MnSiO_4/C is calculated (Fig. 1) to be around 21.2 nm, which is in good agreement with above result in HR-TEM images. It is worth noting that a very thin and uniform carbon layer with the thickness of 3–8 nm is clearly seen on the surface of Li_2MnSiO_4 particle from Fig. 3(e and f). N_2 adsorption–desorption measurement was investigated. The Brunauer–Emmett–Teller (BET) surface area is calculated to be 70.3 m^2 g^{-1}. Apparently, the well distributed fine particles promise large surface area, resulting in short lithium ion diffusion path and enough contact between the active material and electrolyte. Therefore, such uniform carbon layer, as well as limited particle size, will greatly contribute to the lithium ion insertion/extraction. Generally, ball milling was utilized for carbon coating by mixing the precursor and carbon source, wherein the aggregation often took place, which in turn provided the heterogeneous coating effect. In this contribution, phenolic resin, together with related raw materials was firstly dissolved in ethanol with the aim of achieving homogeneous coating. Meantime, phenolic resin in the solution could effectively restrict the aggregation of the precursor. Therefore, Li_2MnSiO_4/C (RF) by *in-situ*

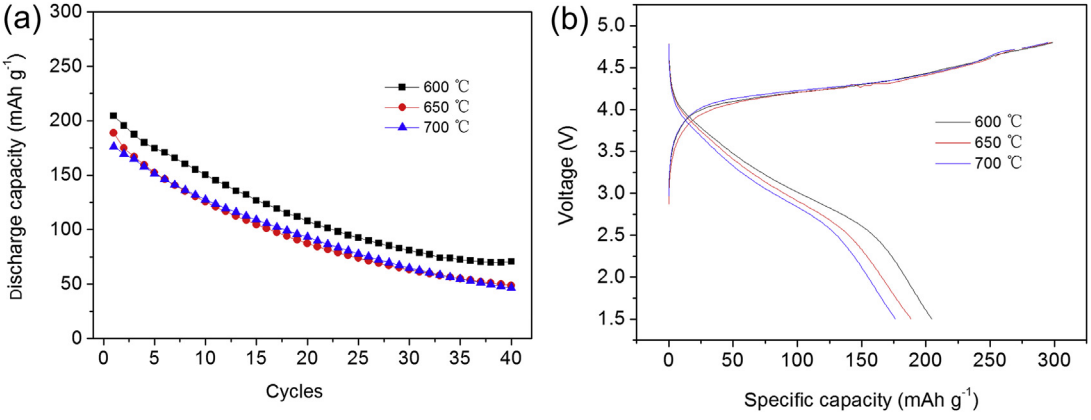

Fig. 2. Cycling performance (a) and the corresponding initial charge–discharge curves (b) of Li_2MnSiO_4/C (RF) composites sintered at different temperatures at a current density of 30 mA g^{-1} between 1.5 and 4.8 V.

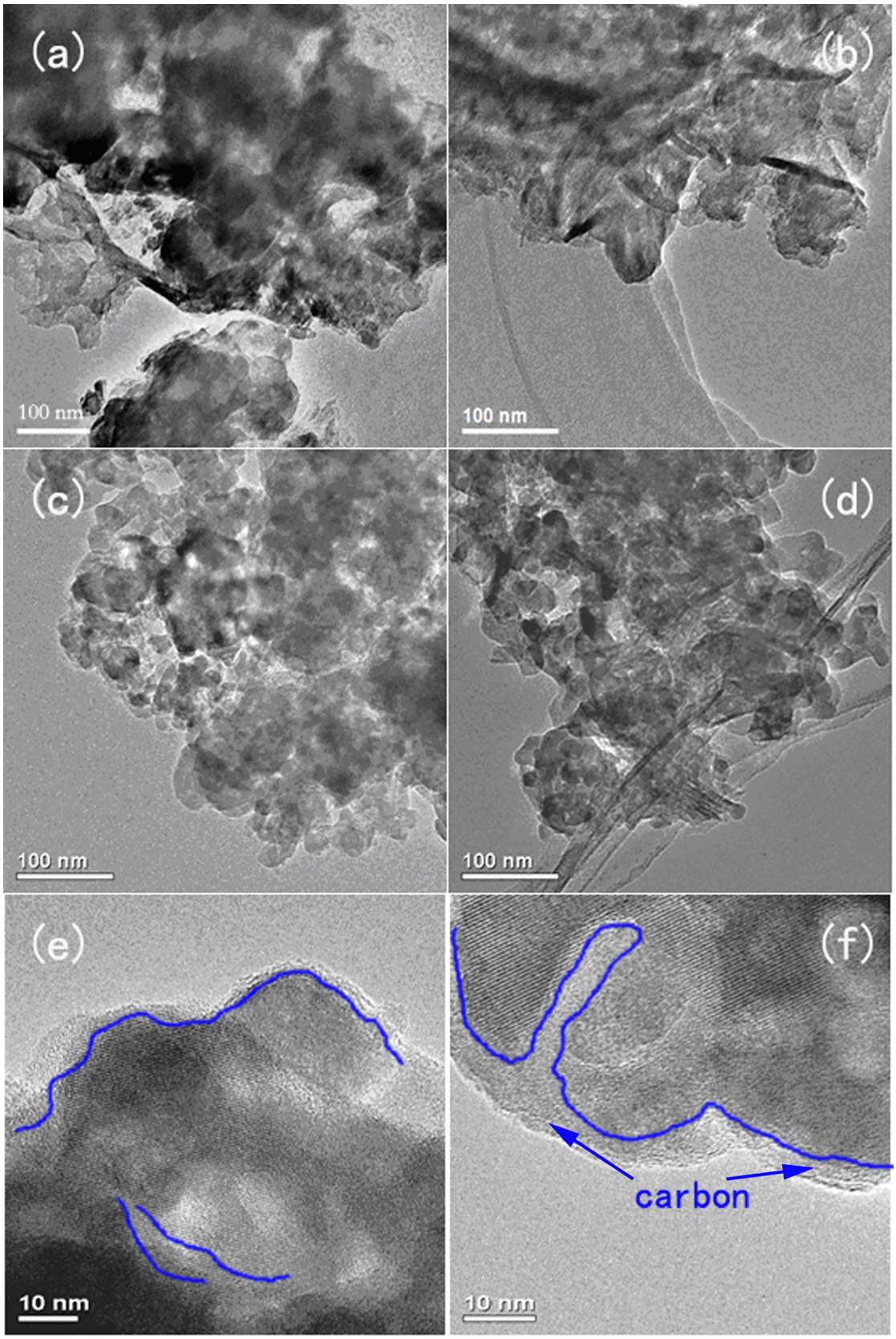

Fig. 3. TEM images of as-prepared Li_2MnSiO_4/C (SR) (a, b) and Li_2MnSiO_4/C (RF) (c, d) composites; HR-TEM images (e, f) of Li_2MnSiO_4/C (RF).

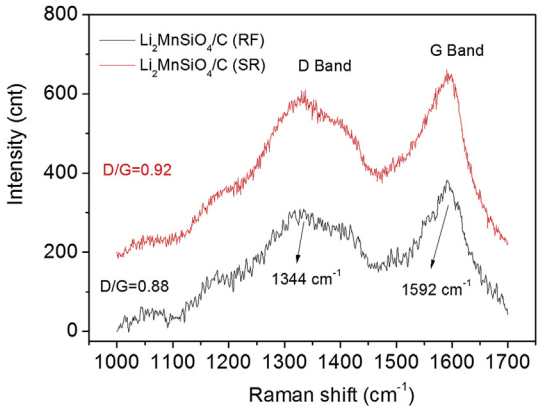

Fig. 4. Raman spectra of as-prepared Li_2MnSiO_4/C (SR) and Li_2MnSiO_4/C (RF) composites.

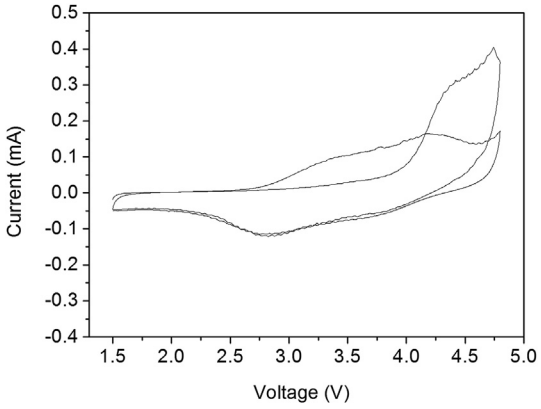

Fig. 5. Cyclic voltammetry curves of as-prepared Li_2MnSiO_4/C (RF) at 0.1 mV s^{-1}.

coating approach is favorable for enhancing electrochemical performance.

Fig. 4 shows the Raman spectra of Li_2MnSiO_4/C (RF) and Li_2MnSiO_4/C (SR) composites. The band in the range of 1150–1450 cm^{-1} (centered on 1344 cm^{-1}) is attributed to the D-band of carbon, which is indicative of the sp^2 disordered induced phonon mode, while that centered on 1592 cm^{-1} is due to the G-band (sp^2 graphite band) [32,40,41]. It is well known that structure of the carbon, particularly the sp^2/sp^3 character, strongly influences the electronic conductivity [31,32]. Generally, electrode materials containing less amounts of high quality carbon i.e., those with high sp^2/sp^3 can outperform those containing larger amounts of a less conductive coating layer. Accordingly, the integral intensity ratios of the D band to the G band for Li_2MnSiO_4/C (SR) and Li_2MnSiO_4/C (RF) are estimated to be about 0.92 and 0.88, respectively. The lower D/G ratio of carbon for Li_2MnSiO_4/C (RF) implies that it should have better electronic conductivity than Li_2MnSiO_4/C (SR). Thus, phenolic resin might be utilized as one kind of high quality carbon source since more highly graphitized carbons are formed during pyrolysis [31]. The electronic conductivities for samples using phenolic resin or sucrose as carbon sources are further measured to approve the Raman results. The value of Li_2MnSiO_4/C using phenolic resin as carbon source is calculated to be 5.2×10^{-2} S m^{-1}, about two orders of magnitude higher than that using sucrose (3×10^{-4} S m^{-1}). The related results provide clear evidence for the merit of phenolic resin as carbon source, which is probably due to the nature carbon quality and the well distribution of carbon coated layer.

Cyclic voltammetry curves (Fig. 5) of as-prepared Li_2MnSiO_4/C (RF) are investigated at a scan rate of 0.1 mV s^{-1}. Much difference of the first two CV curves is observed. For the 1st CV curve, the main oxidation peaks appear at 4.41 and 4.74 V and the corresponding reduction peak is located at 2.83 and 3.81 V. The oxidation peaks in the 2nd CV curve shift obviously toward the low voltage, which is in the range of 2.75 and 4.5 V, while there is almost no change for the reduction peak. The oxidation and reduction peaks are associated with the lithium extraction/insertion behavior, suggesting the probably complicated structure rearrangement of Li_2MnSiO_4 in the first two cycles [15].

Fig. 6 gives the relationships of discharge capacity as a function of cycling numbers for as-prepared Li_2MnSiO_4/C (RF) and Li_2MnSiO_4/C (SR) between 1.5 and 4.8 V at 30 mA g^{-1}. Li_2MnSiO_4/C (RF) exhibits an initial discharge capacity of 204.5 mAh g^{-1} and large capacity loss in the first 20 cycles. With the cycles going on, a capacity-jump, reaching 94.1 mAh g^{-1} is observed after 40 cycles. After that, it gradually decreases to a stable value of 31 mAh g^{-1}. Much poorer electrochemical property is displayed for Li_2MnSiO_4/C (SR), with the maximum discharge capacity of 94.0 mAh g^{-1} and only 32.2 mAh g^{-1} capacity remaining at the 30th cycle. It is apparent that the poorer electrochemical property of Li_2MnSiO_4/C (SR) is due to the inhomogeneous carbon layer and larger particle

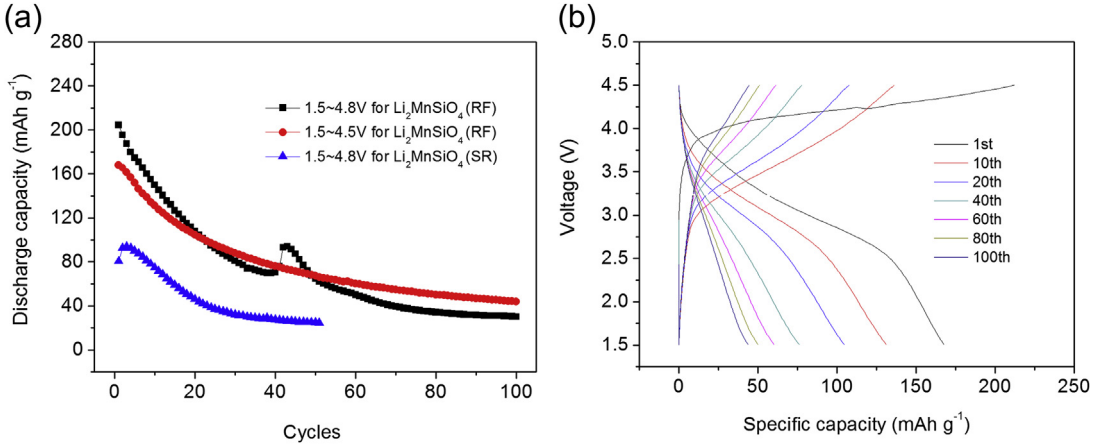

Fig. 6. (a) Cycling performance of as-prepared Li_2MnSiO_4/C (RF) and Li_2MnSiO_4/C (SR) composites between 1.5 and 4.8 V at a current density of 30 mA g^{-1}, associated with cycling performance of Li_2MnSiO_4/C (RF) between 1.5 and 4.5 V; (b) load curves of as-prepared Li_2MnSiO_4/C (RF) composite between 1.5 and 4.5 V at a current density of 30 mA g^{-1}.

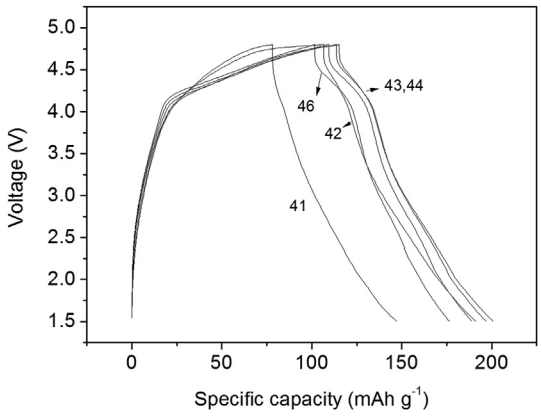

Fig. 7. The 41st–46th load curves of as-prepared Li_2MnSiO_4/C (RF) composite between 1.5 and 4.8 V at a current density of 30 mA g^{-1}.

size, which would result in inferior electronic conductivity and sluggish lithium ion diffusion [25]. Note that the capacity-jump for Li_2MnSiO_4/C (RF) should be associated with the slight structural rearrangement, as verified by the charge–discharge curves in Fig. 7. As shown, at the 41st cycle, the charge plateau is extended and the corresponding discharge curve exhibits a small voltage plateau between 4.1 and 4.5 V. Considering that deep lithium ion extraction from the host would harm the crystal structure and lead to the instability of the electrolyte when charging to 4.8 V, cycling performance with the cut-off voltage of 4.5 V was also investigated (Fig. 6). Although the discharge capacity decreases to 167.8 mAh g^{-1}, the cycling stability of Li_2MnSiO_4/C (RF) electrode is much improved, with the capacity of 44.1 mAh g^{-1} remaining after 100 cycles. Meanwhile, no capacity-jump is observed. Anyway, as those in most of reports, the cycling life of Li_2MnSiO_4/C (RF) in this paper is not good. Yang et al. [42] reported Li_2MnSiO_4/C composites with limited cycling life to 10. In their another work, the capacity of Li_2MnSiO_4/C composite decreased sharply from 209 mAh g^{-1} to 140 mAh g^{-1} after 10 cycles [22]. Belharouak et al. [39] presented an initial discharge capacity of 190 mAh g^{-1} for Li_2MnSiO_4/C, but only 98 mAh g^{-1} remaining after 15 cycles. Manthiram et al. [26] showed that Li_2MnSiO_4/C by micro-wave solvothermal method only retained 50% of its initial discharge capacity at room temperature after 20 cycles. Fig. 8 shows the XRD patterns of Li_2MnSiO_4/C electrode at different charge/discharge states, which provides the evidence from crystal structure into amorphous phase after lithium ions extraction/insertion. The XRD pattern result after cycling is basically consistent with that reported by Yang et al. [22]. Based on the literature, the poor cycling performance of Li_2MnSiO_4/C is probably ascribed to the dynamic Jahn–Teller distortion and structural instability [22,26].

Rate capability of as-prepared Li_2MnSiO_4/C (RF) composite was conducted to ensure the effect of *in-situ* carbon coating. Fig. 9 gives the charge–discharge curves from 0.1 to 5.0 C. As shown, Li_2MnSiO_4/C (RF) electrode delivers the discharge capacities of 205.7, 181.6, 149.1, 133.5 mAh g^{-1} at 0.1, 0.4, 1.2 and 2 C, respectively. Even at 4 and 5 C-rate, the electrode still maintains the discharge capacities of 108.7 and 99.7 mAh g^{-1}, around 52.5% and 48.5% of its capacity at 0.1 C, respectively. To our knowledge, Li_2MnSiO_4/C (RF) here exhibits the best rate performance among those reports so far. Keeping in mind that only a few papers involves the rate capability study for Li_2MnSiO_4/C owing to its poor electronic conductivity. Most of work is focused on the strategies to achieve the higher reversible capacity and cycling stability. Yang and co-workers reported the synthesis of Li_2MnSiO_4/C by two-step carbon coating approach, which exhibited an initial discharge capacity of 209 mAh g^{-1} at 5 mA g^{-1}, however, it decreased to 135 mAh g^{-1} at 150 mA g^{-1} [22]. Manthiram et al. [26] prepared Li_2MnSiO_4/C composite by calcining the mixture of the precursor and sucrose, with the 40% of initial capacity retaining on going from C/50 to 2 C rate. Their discharge capacity at 2 C was less than 100 mAh g^{-1}. Li_2MnSiO_4/C composite having 42% of carbon by V. Aravindan et al. [43] delivered the discharge capacity of 143 and 90 mAh g^{-1} at 0.05 and 1 C, respectively. Since too much carbon coating would reduce the reversible capacity and affect the application of the electrode, strategies to achieve a thin and homogeneous carbon layer with high electronic conductivity in this work are preferable, which has facilitated the improvement of electrochemical properties. Accordingly, the superior rate performance of Li_2MnSiO_4/C in this work should be resulted from the following reasons: (1) *in-situ* coating approach allows the thin and homogeneous layers on the surface of Li_2MnSiO_4 and keeps the particles in good dispersion; (2) Li_2MnSiO_4 crystal growth is effectively limited to a favorable size (*ca.* 25 nm) due to the one-step coating; (3) the carbon layer with low D/G ratios (high sp^2/sp^3) from phenolic resin benefits the improvement of electronic conductivity. Although the cycling stability of as-prepared Li_2MnSiO_4/C in this work was not considerably enhanced, the *in-situ* carbon coating strategy, leading to the superior rate performance, could provide an important clue for significant improvement of electrochemical properties for Li_2MSiO_4 (M = Mn, Fe, Co, etc) in the near future.

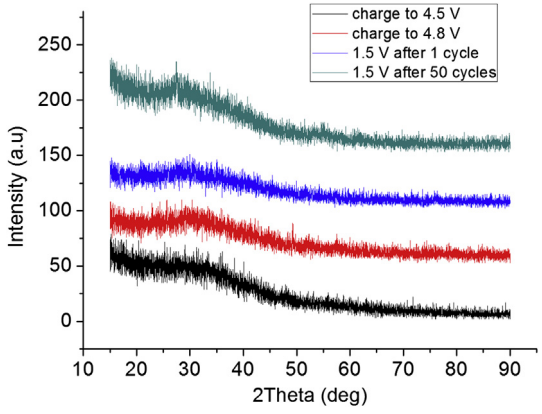

Fig. 8. XRD patterns of Li_2MnSiO_4/C (RF) electrode at different states (charge to 4.5 V; charge to 4.8 V; discharge to 1.5 V after 1 cycle; discharge to 1.5 V after 50 cycles).

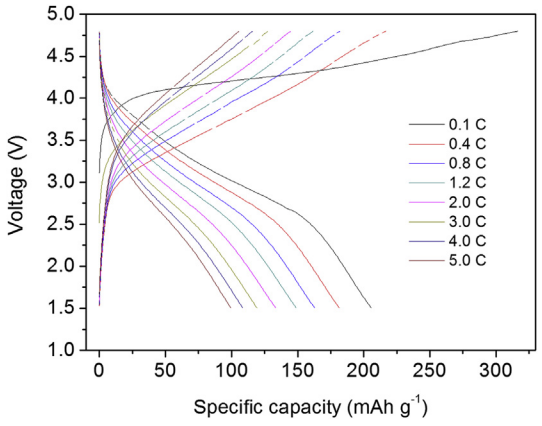

Fig. 9. Load curves of as-prepared Li_2MnSiO_4/C (RF) composite between 1.5 and 4.8 V at various current densities from 0.1 to 5.0 C (1 C = 300 mA g^{-1}).

4. Conclusions

In summary, well dispersed Li_2MnSiO_4/C composites with thin and homogeneous carbon layer were synthesized using phenolic resin as carbon source by *in-situ* coating approach. The average diameter of as-prepared particles was *ca.* 25 nm. In comparison with that using sucrose as carbon source by two-step method, Li_2MnSiO_4/C composites delivered much better electrochemical performance, particularly the rate performance. Even at 4 and 5 C, the discharge capacities of 108.7, 99.7 mAh g^{-1}, around 52.5% and 48.5% of its capacity at 0.1 C were maintained, respectively. It is convinced that the thin and homogeneous carbon layer with high sp^2/sp^3 ratio greatly contributes to high conductivity, thus leading to the superior rate capability. To our knowledge, Li_2MnSiO_4/C composite in this paper shows the best rate performance over the related reports. The *in-situ* carbon coating strategy here could provide an effective approach for synthesizing high performance Li_2MSiO_4/C composites (M = Mn, Fe, Co).

Acknowledgments

The authors greatly appreciate the financial support from the National Nature Science Foundation of China (No. 21271187), China Postdoctoral Science Foundation Funded Project (No. 2013M530356), Scientific Research Foundation of Central South University, Postdoctoral Research Fund of Central South University (No. 7434101 5820) and Scientific Research Foundation of Key Laboratory of Resources Chemistry of Nonferrous Metals of Ministry of Education (No. 2012KF01). Some experiments were done in Prof. Peter G Bruce's group, University of St. Andrews. Dr Haiyan Wang is greatly thankful to Prof. Bruce for his supervision and the financial support.

References

[1] M.S. Whittingham, Chemical Reviews 104 (2004) 4271–4301.
[2] C. Liu, F. Li, L.-P. Ma, H.-M. Cheng, Advanced Materials 22 (2010) E28–E62.
[3] Z. Gong, Y. Yang, Energy & Environmental Science 4 (2011) 3223–3242.
[4] H. Wang, K. Huang, Y. Ren, X. Huang, S. Liu, W. Wang, Journal of Power Sources 196 (2011) 9786–9791.
[5] H. Wang, S. Liu, Y. Ren, W. Wang, A. Tang, Energy & Environmental Science 5 (2012) 6173–6179.
[6] H. Li, Z. Wang, L. Chen, X. Huang, Advanced Materials 21 (2009) 4593–4607.
[7] Y. Wang, P. He, H. Zhou, Energy & Environmental Science 4 (2011) 805–817.
[8] R. Dominko, Journal of Power Sources 184 (2008) 462–468.
[9] J. Gaubicher, C. Wurm, G. Goward, C. Masquelier, L. Nazar, Chemistry of Materials 12 (2000) 3240–3242.
[10] S. Franger, F. Le Cras, C. Bourbon, H. Rouault, Electrochemical and Solid State Letters 5 (2002) A231–A233.
[11] M.R. Roberts, G. Vitins, J.R. Owen, Journal of Power Sources 179 (2008) 754–762.
[12] S.Q. Shi, L.J. Liu, C.Y. Ouyang, D.S. Wang, Z.X. Wang, L.Q. Chen, X.J. Huang, Physical Review B 68 (2003) 195108–195112.
[13] H. Yang, X.L. Wu, M.H. Cao, Y.G. Guo, Journal of Physical Chemistry C 113 (2009) 3345–3351.
[14] A. Nyten, A. Abouimrane, M. Armand, T. Gustafsson, J.O. Thomas, Electrochemistry Communications 7 (2005) 156–160.
[15] R. Dominko, M. Bele, A. Kokalj, M. Gaberscek, J. Jamnik, Journal of Power Sources 174 (2007) 457–461.
[16] C. Lyness, B. Delobel, A.R. Armstrong, P.G. Bruce, Chemical Communications (2007) 4890–4892.
[17] C. Sirisopanaporn, C. Masquelier, P.G. Bruce, A.R. Armstrong, R. Dominko, Journal of the American Chemical Society 133 (2011) 1263–1265.
[18] X. Huang, X. Li, H. Wang, Z. Pan, M. Qu, Z. Yu, Solid State Ionics 181 (2010) 1451–1455.
[19] V. Aravindan, K. Karthikeyan, S. Ravi, S. Amaresh, W.S. Kim, Y.S. Lee, Journal of Materials Chemistry 20 (2010) 7340–7343.
[20] M. Kuezma, S. Devaraj, P. Balaya, Journal of Materials Chemistry 22 (2012) 21279–21284.
[21] V. Aravindan, K. Karthikeyan, J.W. Lee, S. Madhavi, Y.S. Lee, Journal of Physics D – Applied Physics 44 (2011) 152001–152004.
[22] Y.-X. Li, Z.-L. Gong, Y. Yang, Journal of Power Sources 174 (2007) 528–532.
[23] A. Kojima, T. Kojima, M. Tabuchi, T. Sakai, Journal of the Electrochemical Society 159 (2012) A532–A537.
[24] D. Rangappa, K.D. Murukanahally, T. Tomai, A. Unemoto, I. Honma, Nano Letters 12 (2012) 1146–1151.
[25] R. Dominko, M. Bele, M. Gaberscek, A. Meden, M. Remskar, J. Jamnik, Electrochemistry Communications 8 (2006) 217–222.
[26] T. Muraliganth, K.R. Stroukoff, A. Manthiram, Chemistry of Materials 22 (2010) 5754–5761.
[27] Z.-Y. Chen, H.-L. Zhu, S. Ji, R. Fakir, V. Linkov, Solid State Ionics 179 (2008) 1810–1815.
[28] Y.-D. Cho, G.T.-K. Fey, H.-M. Kao, Journal of Power Sources 189 (2009) 256–262.
[29] J.D. Wilcox, M.M. Doeff, M. Marcinek, R. Kostecki, Journal of the Electrochemical Society 154 (2007) A389–A395.
[30] X. Zhi, G. Liang, L. Wang, X. Ou, L. Gao, X. Jie, Journal of Alloys and Compounds 503 (2010) 370–374.
[31] M.M. Doeff, Y.Q. Hu, F. McLarnon, R. Kostecki, Electrochemical and Solid State Letters 6 (2003) A207–A209.
[32] Y.Q. Hu, M.M. Doeff, R. Kostecki, R. Finones, Journal of the Electrochemical Society 151 (2004) A1279–A1285.
[33] H.-M. Xie, R.-S. Wang, J.-R. Ying, L.-Y. Zhang, A.F. Jalbout, H.-Y. Yu, G.-L. Yang, X.-M. Pan, Z.-M. Su, Advanced Materials 18 (2006) 2609–2613.
[34] P.G. Bruce, B. Scrosati, J.-M. Tarascon, Angewandte Chemie International Edition 47 (2008) 2930–2946.
[35] M.E. Arroyo-deDompablo, R. Dominko, J.M. Gallardo-Amores, L. Dupont, G. Mali, H. Ehrenberg, J. Jamnik, E. Moran, Chemistry of Materials 20 (2008) 5574–5584.
[36] V.V. Politaev, A.A. Petrenko, V.B. Nalbandyan, B.S. Medvedev, E.S. Shvetsova, Journal of Solid State Chemistry 180 (2007) 1045–1050.
[37] C. Sirisopanaporn, R. Dominko, C. Masquelier, A.R. Armstrong, G. Mali, P.G. Bruce, Journal of Materials Chemistry 21 (2011) 17823–17831.
[38] G. Zhong, Y. Li, P. Yan, Z. Liu, M. Xie, H. Lin, Journal of Physical Chemistry C 114 (2010) 3693–3700.
[39] I. Belharouak, A. Abouimrane, K. Amine, Journal of Physical Chemistry C 113 (2009) 20733–20737.
[40] C.-W. Ong, Y.-K. Lin, J.-S. Chen, Journal of the Electrochemical Society 154 (2007) A527–A533.
[41] M. Maccario, L. Croguennec, B. Desbat, M. Couzi, F. Le Cras, L. Servant, Journal of the Electrochemical Society 155 (2008) A879–A886.
[42] W. Liu, Y. Xu, R. Yang, Journal of Alloys and Compounds 480 (2009) L1–L4.
[43] V. Aravindan, K. Karthikeyan, K.S. Kang, W.S. Yoon, W.S. Kim, Y.S. Lee, Journal of Materials Chemistry 21 (2011) 2470–2475.